Pregnane X Receptor Activation Induces Fibroblast Growth Factor19 Dependent Tumor Aggressiveness in Humans and Mice

Hongwei Wang, Madhukumar Venkatesh, Hao Li, Regina Goetz, Subhajit Mukherjee, Arunima Biswas, Liang Zhu, Andreas Kaubisch, Lei Wang, James Pullman, Kathleen Whitney, Makoto Kuro-o, Andres I. Roig, Jerry W. Shay, Moosa Mohammadi and Sridhar Mani

This file includes:

Supplemental Methods, including primer sequences and shRNA sequences

Supplemental Table 1- 2

Supplemental Figures 1 – 11

Supplemental References

Supplemental methods

Cell lines, tumor tissues and Reagents. The human colon cancer cell lines LS174T, Caco-2, LoVo, HCT116, SW948, SW403, and HEK 293T cells were from the American Type Culture Collection (ATCC) and cultured according to ATCC recommendations. HIEC, a human intestinal epithelial crypt cell line, and its appropriate growth media were provided by Dr. Jean-Francois Beaulieu, University of Sherbrooke, Quebec, CN (1). Surgically resected human colon tumor tissues and Paraffin-embedded colon cancer tissues were obtained from the Department of Pathology, Montefiore Medical Center. Paraffin-embedded colon cancer tissue array (CO801) was obtained from US Biomax, Inc. Charcoal adsorbed fetal bovine serum (FBS), DMSO, pregnenolone carbonitrile (PCN), puromycin, rifampicin, epidermal growth factor (EGF), hydrocortisone, Insulin, transferring and sodium selenite were from Sigma Aldrich; Hoechst 33258 from Molecular Probes (Invitrogen); Hematoxylin & Eosin stain from Poly Scientific; Trypan blue stain and medium 199 are from GIBCO BRL (Invitrogen). Expression and purification of human FGF19 (residues R23 to K216) and the FGF23 antagonist has been carried as previously described (2, 3). Recombinant human FGF23 is from R&D systems (2604-FG). The FGF19 antibody 1A6 and FGF19 peptide (4) was provided by Dorothy French, Genentech, Inc. PXR antibody was available from Dr. R.K.Tyagi, Jawaharlal Nehru University, New Delhi, India and the antibody used for immunohistochemistry was from BioLegend Inc. (5). For ChIP assay, PXR antibody (sc-25381) was obtained from Santa Cruz Biotechnology. Other antibodies used are as indicated: BrdU antibody (Calbiochem, # JA1599), CEA (Invitrogen, # 08-1013), FGF19 (sc-16831, N-20 and sc-73984, W12), ERK (total, sc-93, C-16), phospho ERK (sc-7383, E-4), FRS2α (sc-8318, H-91), phospho

FRS2α (Cell Signaling, #3864), nonspecific rabbit IgG (sc-2027), β-actin (Abcam, #ab8227), GAPDH (sc-25778). PXR (RP11-169N13) and FGF19 (RP-11-30016) BAC clones were obtained from www.bacpac.chori.org. pEGFPC1 (Clontech) vector and GFP-human PXR were kind gifts from Dr. J Kim Kemper (Department of Molecular and Integrative Physiology, School of Molecular and Cellular Biology, University of Illinois, Urbana, Illinois ,U.S.A.) (6). ^{32}p-ATP 250 μci (NEG502Z250) was obtained from Perkin Elmer. RNA polymerase II kit was purchased from SA Biosciences Corporation.

Cell proliferation assays (doubling time). Tryphan blue exclusion and BrdU cell proliferation assays are described in supplemental methods. 24-well plastic plates (flat bottom) were seeded with 15,000 viable cells/well. Cell viability was determined by trypan blue exclusion and counting with both hemocytometer and Vi-cell XR cell viability analyzer (Beckman Coulter). 6 hours post seeding, cells were harvested by trypsin digestion for repeated counting on day 1 (24 hours post seeding), day 2 (48 hours) and day 3 (72 hours). Growth rate constants were calculated using the formula, k = ln2/g, where ln 2 is the natural logarithm of 2 and "g" is the time in hours taken for the population to double during the exponential phase of growth within 72 hours from initial seeding. The BrdU Cell Proliferation assay was performed according to the manufacturer's instructions (Calbiochem). Briefly, 96 well plates were seeded with 50,000 cells/well. After 24 hours cells were treated with vehicle/rifampicin (0-50μM) for 48 hours. Subsequently, during final 4 hours of culture, BrdU was added to the wells of the plate. After the incubation period, cells were fixed, permeabilized, DNA denatured and processed according to the manufacturer's instructions. BrdU incorporation in cells (nuclei) was measured as spectrophotometric absorbance at dual wavelength of 450-550 nm.

Chromatin Accessibility by Real-Time PCR (CHART-PCR) assay. LS174T and HIEC were treated for 48 hours with either rifampicin (10μM) or vehicle (0.2% DMSO), and then pelleted by centrifugation at 4˚C. 5 x 10^6 cells/sample were washed once with ice-cold PBS (pH 7.4) and then re-suspended for 5 min in ice-cold lysis buffer (10 mM Tris (pH 7.4), 10 mM NaCl, 3 mM $MgCl_2$, 0.5% Nonidet P-40, 0.15 mM spermine and 0.5 mM spermidine). The cell nuclei were pelleted and washed twice with the buffer for *Xho*I digestion (without $CaCl_2$), and restriction assays were performed as previously published (7). As a control for endogenous endonuclease activity, samples of cells from each treatment group to which no *Xho*I enzyme had been added were included in the assay. For the CHART-qPCR assay, DNA of the samples from the accessibility assay was quantified using a NanoDrop 1000 spectrophotometer. 50 ng of genomic DNA were used to perform SYBR Green Real-Time PCR. The PCR was performed in 10 μl reaction volumes according to the manufacturer's instructions (7900HT, Applied biosystems (AB)) (8). Each PCR reaction was run in triplicate and for each primer set, four separate experiments were run. To correlate Ct values (threshold values) from FGF19 CHART-PCR amplification plots to percent accessibility, a standard curve was generated using serial dilutions of genomic DNA and the appropriate primer sets, using previously published methods (7). The concentration data were calculated and plotted as a percentage of undigested samples for each cell treatment. The primer sets A-C (Supplemental Table 1) were developed and tested for use in CHART-qPCR across the FGF19 proximal promoter (within –3.0kb from the transcription start site). However, only primer sets A (slope – 3.33 and r^2 = 0.985; single peak on association/dissociation curve) had ideal parameters for qPCR analysis. As an additional control, an unrelated primer set D (> -50kb from transcription start) was used

to amplify *Eco*RI-digested genomic DNA from all experimental samples (Supplemental Table 1). As expected, there was no difference in *Eco*RI site accessibility between all samples (data not shown).

***Immunoblotting*.** Cell lysate was separated by SDS-PAGE and analyzed by immunoblotting as previously published (5). Antibodies used in these studies were as follows FGF19 (W12, sc-73984, Santa Cruz.; 1:1000), PXR antibody (sc-25381, Santa Cruz Biotechnology Inc.; 1:1000), p-ERK (sc-7383, E-4, Santa Cruz Biotechnology Inc.; 1: 2000), ERK (sc-93, C-16, Santa Cruz Biotechnology Inc.; 1: 5000) and β-actin (#ab8227, Abcam Inc.; 1:5000). β-actin was used to normalize the data for protein loading. After being incubated with horseradish peroxidase-conjugated secondary antibody, the proteins bound to the membrane were visualized using ECL method (GE Healthcare). The intensity of the protein bands on the membrane were quantified using Image J software (NIH, http://rsb.info.nih.gov/ij/).

***Transwell migration assay*.** Cells were grown in 6-well plates in the presence or absence of rifampicin (25μM) for 48 hours. Subsequently, 10^4 cells/well were seeded onto a 96-well chemotaxis chamber (MBA96; Neuroprobe Inc.) fitted with polycarbonate filters (PFD8/A; 8 μm pore size). Rifampicin (25μM) or DMSO (0.2%) (Negative or untreated control) or EGF (5nM) (positive control) or FGF19 (1000 ng/ml) and/or FGF19 inhibitor (400 ng/ml) or FGF23 (400 ng/ml), each diluted in serum-free media, was added to the top and bottom chamber of each well, and cells were analyzed from the bottom wells at 12 and 24 hours time points. The number of migrated cells was measured by adding MTS reagent and measuring MTS absorbance. Cell inoculation and counting were carried out exactly as

described by the manufacturer (Neuroprobe, Inc). Based on repeated control migration experiments (that included 48 hours and 72 hours time points), we found that by 24 hours cell migration had reached its maximum (data not shown). At 24h, the EGF well MTS absorbance was normalized to a single EGF well (x 100) which was considered as 100% migration. Percent migration was obtained for all corresponding MTS readings from treated (t) and untreated (ut) wells using the formula - [MTS reading]t or [MTS reading]ut /[corresponding EGF well MTS reading] x 100.

***In Vivo Experiments*.** The mice strains used were C57BL/6 mice (6-8 weeks old) and, athymic Balb/c nu/nu mice (B6.Cg-Fox1<nu>/JALT1) from Jackson Laboratory. *pxr* $^{-/-}$ mice were the kind gift from Dr. Wen Xie, University of Pittsburgh. For tumor growth studies, 5 x 10^6 cells [Scrambled or control shRNA, PXR and FGF19 shRNA (Open Biosystems) transduced LS174T cells] were implanted in both flanks of athymic Balb/c nu/nu mice. After 14-22 days (average of 20 days), when tumors were clinically detectable and small (~25mm^3), mice were randomly allocated by tumor size criteria to two treatment groups: a) control group receiving 30% polyethylene glycol (3x per week) intravenously and b) rifampicin, 40 mg/kg (3x per week) intravenously. The tumor size was measured and calculated at the indicated time-points (Figure 1B) as previously published (5).

Human tumor heterotransplant experiments. For human tumor heterotransplant experiments, using a single primary human tumor specimen, tumors were passaged serially twice or more times to expand the animal numbers and normalize starting tumor volumes ~ ~25mm^3 (reached at approximately day 7 from grafting). Animals were then equally distributed (by tumor volumes) to treatment groups. (i) Mice treated with: (1) control

antibody (20mg/kg intraperitoneal two times per week) (4), (2) control peptide (intratumoral injection, 1 mg/kg two times/day), (3) Rifampicin (40 mg/kg/day intravenously for 3 consecutive days/week) + control antibody, (4) Rifampicin + control peptide, (5) Rifampicin + FGF19 neutralizing antibody (1A6; 20mg/kg intraperitoneal two times per week) (4), (6) FGF19 protein (intratumoral injection, 1 mg/kg two times/day) + control antibody, (7) FGF19 protein + FGF19 antibody, and (8) FGF19 antibody + control peptide. The treatment duration was for 35 days from tumor inoculation. (ii) Mice treated with vehicle (30% polyethylene glycol) or rifampicin (Rif) 40 mg/kg/day intravenously for 3 consecutive days (3 weeks). Then total RNA was isolated from the treated tumor tissues and subsequently cDNA synthesis and quantitative RT-PCR carried out as described above. (iii) Mice treated with (1) vehicle (30% polyethylene glycol) (2) rifampicin (Rif) 40 mg/kg/day intravenously for 3 consecutive days or (3) FGF19 antibody (1A6; 20mg/kg i.p. two times per week) (4) rifampicin (Rif) and FGF19 antibody (1A6; 20mg/kg i.p. two times per week). Isolated human colon tumors (n=3 pooled) (3 weeks) were sonicated and tissue was used for electrochemiluminescence assay with antibodies directed against pERK/ERK and pFRS2/FRS2.

In vivo liver metastasis. Briefly, athymic Balb/c nu/nu mice were inoculated with 1 x 10^6 LS174T carcinoma cells through intrasplenic injection. In the initial set, 24 animals/group (scrambled shRNA transduced LS174T cells and PXR shRNA transduced LS174T cells) were inoculated (12, vehicle controls and 12, rifampicin-treated with 40 mg/kg IV 4x/ week for 2 weeks). On day 14, the mice were sacrificed, and liver and spleen tissues were isolated for gross and microscopic examination of metastasis (Figure 1E & G). Thereafter, quantitation of surface and microscopic hepatic nodules was performed on day 14.

DNA methylation. For this purpose, the MethPrimer program (9) was used to scan for CpG islands and design primers across a 2kb region upstream of the FGF19 promoter initiation start site. Most of the sequence within this 2kb region was not rich in CpG and only two small islands were found with predicted primers for bisulfite-conversion-based methylation PCR. Nevertheless, we designed additional primer pairs for bisulfite PCR across the entire 2 kb region. EZ DNA Methylation kit (Zymo Research) was used for bisulfite conversion of DNA. The methylation profile of the purified, converted DNA (from both LS174T and HIEC) was determined by PCR amplification followed by DNA sequencing (see manufacturer's protocol).

Transient transfection. HIE and HCEC 1CT/2CT (cultured as previously published (10)) cells were transfected with pEGFPC1 (Clontech) vector and GFP-human PXR using solution L, program D-023 (Amaxa Inc.), according to manufacturer's guidelines. After nucleofection the cells were seeded in 100X20 mm plates (BD Biosciences) to culture for 48 hours, then GFP positive cells were assessed and sorted by fluorescence-activated cell sorting (FACS, BD Biosciences). Sorted cells were seeded in 96-well plate for the proliferation assay and 100X20 mm plates to prepare the cell lysate for immunoblot.

RNA preparation and Semi-quantitative RT-PCR (Semi- QPCR). Total RNA was extracted from cells and tumors using the RNeasy Mini kit (Qiagen) and TRIzol (Invitrogen), respectively according to the manufacturer's instructions. 2 μg of total RNA were reverse transcribed with random hexamer primers and SuperScript™ III-RT (Invitrogen). Semi-QPCR was used to assess mRNA expressions of FGF19, MDR1, and GAPDH as previously published (11). For human (h) cell lines, the following PCR

conditions were used: 94˚C for 2 minutes, and then each cycle at 94˚C for 30 seconds, 56˚C for 30 seconds, 74˚C for 30 seconds, repeated for 20 cycles. The final cycle extension time was 10 minutes. GAPDH were used to normalize data. The following primer pairs were used in RT-PCR:

FGF19 (349bp), Forward primer: 5'-GCACAGTTTGCTGGAGATCA-3'

Reverse primer: 5'-GGGCAGGAAATGAGAGAGTG-3'

hGAPDH (349bp), Forward primer: 5'-TGCATCCTGCACCACCAACT-3'

Reverse primer: 5'-CGCCTGCTTCACCACCTTC-3'

hMDR1 (719bp), Forward primer: 5'-TGGTCAGTGTTGATGGACAG-3'

Reverse primer: 5'-ATCCAGAGCCTCTTTGGTAC-3'.

Real-Time Quantitative (Q) PCR. 2.0 μg of total RNA extracted from cells/tumor were reverse transcribed with random hexamer primers and SuperScript™ III-RT (Invitrogen). Taqman PCR (TaqMan universal PCR master mix) reactions were performed in triplicate for each sample and analyzed on the ABI Prism 7900HT system. Data were normalized to β-actin or GAPDH mRNA abundance. RT-quantitative PCR for PXR, FGFs, FGFRs, β*K*lotho, MDR1, GAPDH and β-actin, were performed using TaqMan universal PCR master mix and TaqMan probes using, FAM as the 5' reporter fluorochrome and tetramethylrhodamine (MGB) as the 3' quencher fluorochrome as previously described (5). Primers and minor groove binder/non-fluorescent quencher probes used for PCR amplification were obtained from Applied Biosystems (human β-actin MGB probe with FAM dye label), as well as the following assays on demand: Hs00391591_m1 (FGF19); Hs00184500_ml (MDR1); Hs00242558_m1 (FGFR4); Hs00240792_m1 (FGFR2); Hs00179829_m1 (FGFR3); Hs00545621_m1 [(β*K*lotho (KL)]; Hs00915140_m1 (FGFR1)

Hs01114265_gl (PXR); Mm01344143_g1 (mpxr); Mm00433278_ml (fgf15) Hs00221003_ml (FGF23); Mm99999913_g1 (gapdh) (Applied Biosystems). Controls included RT-minus RNA samples. PCR reaction conditions for all assays were 50°C for 2 minutes, 95°C for 10 minutes, followed by 40 cycles of amplification (95˚C for 15 seconds then 60˚C for 1 minute).

***Lenti-based shRNA knock-down systems*.** For PCR template sequences containing specific target sequences were obtained through the RNAi Codex website (codex.cshl.edu/scripts/newmain.pl), and the chosen sequences are as follows :PXR1.0 TGCTGTTGACAGTGAGCG**CGGCTACGCTGACAATCAGTTA**TAGTGAAGCCAC AGATGTAT**AACTGATTGTCAGCGTAGCCT**TGCCTACTGCCTCGGA, (targets NM_4154….4175), scrambled: tgctgttgacagtgagcgcg**gtactgccgcaatgctata** atagtgaagccacagatgtat**tatagcattgcggcagtacc**ttgcctactgcctcgga, PXR2.0 TGCTGTTGACAGTGAGCG**CGGACCAGATCTCCCTGCTGAA**TAGTGAAGCCAC AGATGTA**TTCAGCAGGGAGATCTGGTCCT**TGCCTACTGCCTCGGA, (targets NM_003889 (2650...2671) scrambled: tgctgttgacagtgagcgcg**gcacaccggtcagcttact** atagtgaagccacagatgtat **agtaagctgaccggtgtgcc**ttgcctactgcctcgga. Bold letter sequences were derived from PXR target gene. PXR 1.0 and 2.0 were chosen after testing five from fifteen possible hairpin sequences. These sequences were cloned into Lenti: CMV–GFP plasmid individually or combined as previously published (12). The best results were obtained with PXR1.0/PXR2.0 combination cloned into a single lentivector (Supplemental Figure 1). The following primers were used to amplify and clone silent PXR mutation for knockdown-rescue assays: (forward) 5’- gac CAGATTTCCCTCTTGAAGgg-3’ and (reverse) 5'- CCC TTC AAG AGG GAA ATC TGG TC -3'. These primer sequences were based on hiRNA

target sequence (underlined) 5' – acCAGATCTCCCTGCTGAAGgg- 3', which corresponds to 6 amino acid residues – Q272, I273, S274, L275, L276, and K277. Based on the likelihood of best hairpin (iRNA) contact, the final predicted nucleotide change (marked in red) that would provide us with at least three silent amino acid mutations was predicted to be 5'- acCAGATTTCCCTCTTGAAGgg- 3' with the corresponding amino acids – I273I, L275L, and L276L being unchanged. The silent mutation was then made according to the manufacturer's instructions of the QuikChange II Site-directed Mutagenesis Kit (Cat# 200523, Stratagene).

For human FGF19 shRNA based knockdown, GIPZ lentiviral shRNAmir's (RHS4531 clone-ID V2LHS_50189, V2LHS_50187, V3LHS_413209) and Non-Silencing control vector were purchased from Open Biosystems. After testing each individual GIPZ shRNAmir, the best combination for FGF19 knockdown was attained using all three clones together (Supplemental Figure 8C). Notably, FGF19 protein rescues loss of FGF19 (Supplemental Figure 8D).

Lenti virus assembly and transduction. 293T cells were cultured in Dulbecco's Modified Eagle Medium (DMEM) supplemented with 10% fetal bovine serum (FBS). Lentivirus were generated through co-transfection of 293T cells with lentiviral plasmids (shRNA against PXR/scrambled PXR or shRNAmir's of FGF19/Non-Silencing Control) and packaging plasmids (pMDLg/pRRE, pRSV-REV, and pMD2-VSVG or Trans-Lentiviral Packaging Mix - pTLA1-Pak, pTLA1-Enz, pTLA1-Env, pTLA1-Rev and pTLA1-TOFF, Open Biosystems) by standard calcium phosphate protocol (12). After 48 h of transfection, supernatant was collected and filtered (0.2 μm pore size). Virus titers were determined by infection of 293T cells with serial dilution of viral stock and the percentage of GFP

positive cells were assessed by FACS. For transduction, LS174T cells were incubated with viral supernatants (shRNA PXR1/2 or scrambled shRNA or shRNAmir's FGF 19/ Non-Silencing Control) for 24 hours at 37°C in the presence of 8 μg/ml of polybrene (Sigma Aldrich). After 3 days, the percentage of GFP-positive cells was determined by fluorescence-activated cell sorting (FACS, BD Biosciences), as previously published (Supplemental Figure 1) (12). GFP positive cells were assessed and sorted by fluorescence-activated cell sorting (FACS, BD Biosciences). GFP-positive cells were cultured and knockdown efficacy was assessed by real-time QPCR and immunoblot.

Chromatin ImmunoPrecipitation (ChIP) assay. We used a fast ChIP method as previously published (13). In fast ChIP method, after cross-linking with formaldehyde, the cells were lysed, and fractions containing nuclear pellets were isolated and chromatin sheared. The chromatin samples were incubated with antibodies in an ultrasonic bath followed by centrifugation to obtain pre-cleared samples. These were mixed with protein 'A' beads. After several washes, Chelex 100 suspension was added to the beads, the suspension was boiled and tubes allowed to cool. After shaking and repeated boiling, the centrifuged samples were analyzed for PCR-ready DNA. Quantitative (q) PCR was used for detection of pull-down chromatin (13). We initially used a 35 cycle PCR to detect interaction but observed non-specific interactions (i.e IgG plus rifampicin-treated samples). Therefore, we performed quantitative PCR as previously published (14). For semi-quantitative PCR (15), and quantitative PCR (16), a 215bp (CYP3A4 ER6 element) and 262bp (putative PXR binding site on FGF19 promoter by TRANSFAC analysis) PCR fragment were amplified. The input reflects 1% of total lysate after sonication. IP controls included H_20 (water) and non-specific IgG (same class as PXR antibody). For PCR

detection, the following primers were used: FGF19 (forward): 5'-AAGAACCTGAGACTGTCGGAACTGC-3', FGF19 (reverse): 5'-ATCAGGCTCCCAGTGGATGCACTC-3'. CYP3A4 (forward): 5'ATGCCAATGGCTCCACTTGAG-3', CYP3A4 (reverse) 5'-CTGGAGCTGCAGCCAGTAGCAG-3'. The PCR conditions included a hot start (95˚C for 3minutes) followed by 35 cycles of 95˚C for 30 seconds, 60˚C for 30 seconds , 72˚C for 30 s , then 72˚C for 3 minutes (extension).

SYBR GreenER^{TM} qPCR SuperMix Universal (Invitrogen) was used for SYBR Green PCR. The conditions for quantitative PCR used were: UDG incubation at 50˚C for 2 minutes, then UDG inactivation at 95˚C for 10 minutes followed by 40 cycles (95°C for 10 s, 60°C for 20 seconds, 72°C for 30°C, then 95°C for 15 seconds, 60°C for 15 seconds 95°C for 15 seconds). Data analysis was performed using the ChIP-qPCR Assay Data Analysis Template (SuperArray, Bioscience Corporation). For PolII-ChIP, the following primers were used: TATA and GCGC Box (+) strand: FGF19 (forward): 5'- TTG CAT CTC GCG CAC AGC CGC G -3'; FGF19 (reverse): 5'- CGG CAG TTC CGA CAG TCT CAG G -3'.

Electrophoretic Mobility Shift Assay (EMSA). The gel shift assays were performed as described previously (11). Briefly, human PXR and RXR were translated in vitro using TNT® T7 Quick Coupled Tanscription/Translation System (Promega). Double stranded oligonucleotides of specific response elements on CYP3A4 and FGF19 were used as probe (Supplemental Table 2). Additionally, cold oligo of FGF19 wild type ER6/DR3 used to compete for PXR binding with labeled probe. The oligonucleotides were synthesized at Invitrogen. These oligonucleotides fragments were labeled with [γ-^{33}P] ATP (Perkin

Elmer) using T4 polynucleotide kinase (New England Labs). Ten (10) μg in vitro translated PXR or RXR or PXR/RXR (1:1) were incubated with the radiolabeled probe in binding buffer (10 mM Tris-Cl, pH 8.0, 150 mM KCl, 0.2 mM dithiothreitol, 0.5 mM EDTA, 14% glycerol) in a final volume of 10 μl for 30 minutes at room temperature. The reaction mixture was then subjected to electrophoresis on a 4 -20% gradient native gel (Bio-Rad). The gel was dried and analyzed by phosphorimager (STORM 860, Molecular Dynamics).

Electrochemiluminescence. MSD's chemiluminescence detection technology (www.mesoscale.com; Gaithersburg, MD) was employed to measure FGF19, ERK, phospho ERK, FRS2α, phospho FRS2α in lysate and/or culture media of LS174T cells after cell stimulation with rifampicin or vehicle control. Cell lysate /extracellular media (0-5 μg) was coated on 96-well MULTI-ARRAY MSD high bind plates according to manufacturer's instructions. The wells were incubated at room temperature for 2 hour, and then blocked with MSD Blocker 'A' solution diluted in PBS for 1 hour at room temperature. After incubation with primary antibody (1 μg/ml) for 1 hour at room temperature, the wells were washed with Blocker 'A' solution and then incubated with the secondary antibody (1 μg/ml). After an additional 1 hour of incubation, the wells were washed and refilled with 150 μl MSD Read Buffer (1x) with surfactant. Readings were measured using the SECTOR Imager 2400 according to manufacturer's instructions. Experiments were performed in duplicate and repeated twice. Anti-ERK1/2 and FRS2α antibody were used to normalize the data for protein loading.

A standard curve was constructed using recombinant FGF19 protein. Various concentrations of FGF19 protein (0-10ng) were coated on to the 96-well MULTI-ARRAY MSD high bind plates according to manufactures guidelines. The experiment was carried out as described above and signals (light units) were plotted against the FGF19 protein concentrations.

Table S1

Primer Sets	Primer sequences (5′ to 3′)	C_t
Set A (XhoI)	**Fwd:** AGC CCA GCA AAC ACC CAA GAT CGT GTG **Rev:** GGA TCC TGC TCA TGT GAG GTA GCT G	18.8
Set B (NcoI)	**Fwd:** TTC ACC ACT AAC AGA GTG TGC GAC CTT GG **Rev:** TTC TCA GCT CAA ATC TCC ACA AGA GCC	19.8
Set C (XbaI)	**Fwd:** CTG AAC CAA GAC ACA CAG CGT GG **Rev:** AGG GCG CAG CAA ATG TCA CCA GGA AAG	20.2
Set D (EcoRI)	**Fwd:** GCT TGG CAG AGG CAA TGA AAG CTA AGA TG **Rev:** CTC TTC TTA TGA GGA CAC CAG TCA CTG	21.2

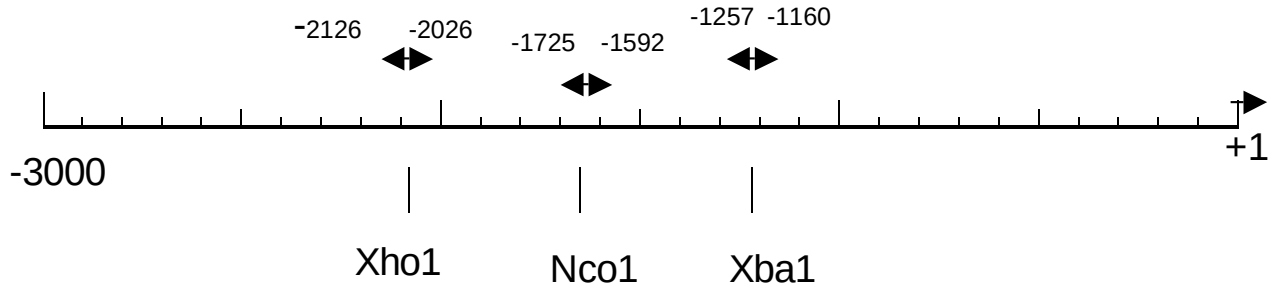

Table S1. Primer sequence for SYBR Green real-time PCR analysis.
(The C_t values were generated from the real–time PCR plots with a threshold value of 0.118. The amount of input genomic DNA was 50ng).

Table S2

Gene	Response element	Oligonucleotide sequence	Nucleotides location
CYP3A4	ER6	-5'-aata*TGAACT*caaagg*AGGTCA*gtga-3' 5' -tcacTGACCTcctttgAG TTCAtatt-3'	-173 to -147
FGF1	ER6	5'-cccg*TGCCCC*acgccg*AGTGCA*tccact-3' 5' - agtggaTGCACTcggcgtGGGGCAcggg-3'	-85 to -57
FGF19 mut1		5'-cccg*GTAAAA*acgccg*AGTGCA*tccact-3' 5'-agtgga TGCACTcggcgtTTTTACcggg-3'	
FGF19 mut2		5'-cccg*TGCCCC*acgccg*CTCTTC*tccact-3' 5'- agtggaGAAGAGcggcgtGGGGCAcggg-3'	
FGF19	DR3	5'- ggaAGGGCActaAGGCCGagg-3' 5'-cctCGGCCTtagTGCCCTtcc-3'	-180 to -159
FGF19 mut1		5'-ggaCTTATGctaAGGCCGagg-3' 5'-cctCGGCCTtagCATAAGtcc-3'	
FGF19 mut2		5'-ggaAGGCActaGAATTAagg-3' 5'-cctTAATTCtagTGCCCTtcc-3'	

Table S2. Table represents oligonucleotide sequence of ER6/DR3 elements on CYP3A4 and FGF19 promoter. Letters in uppercase denote the ER6/DR3 elements. Underlined upper case letters denote the mutation.

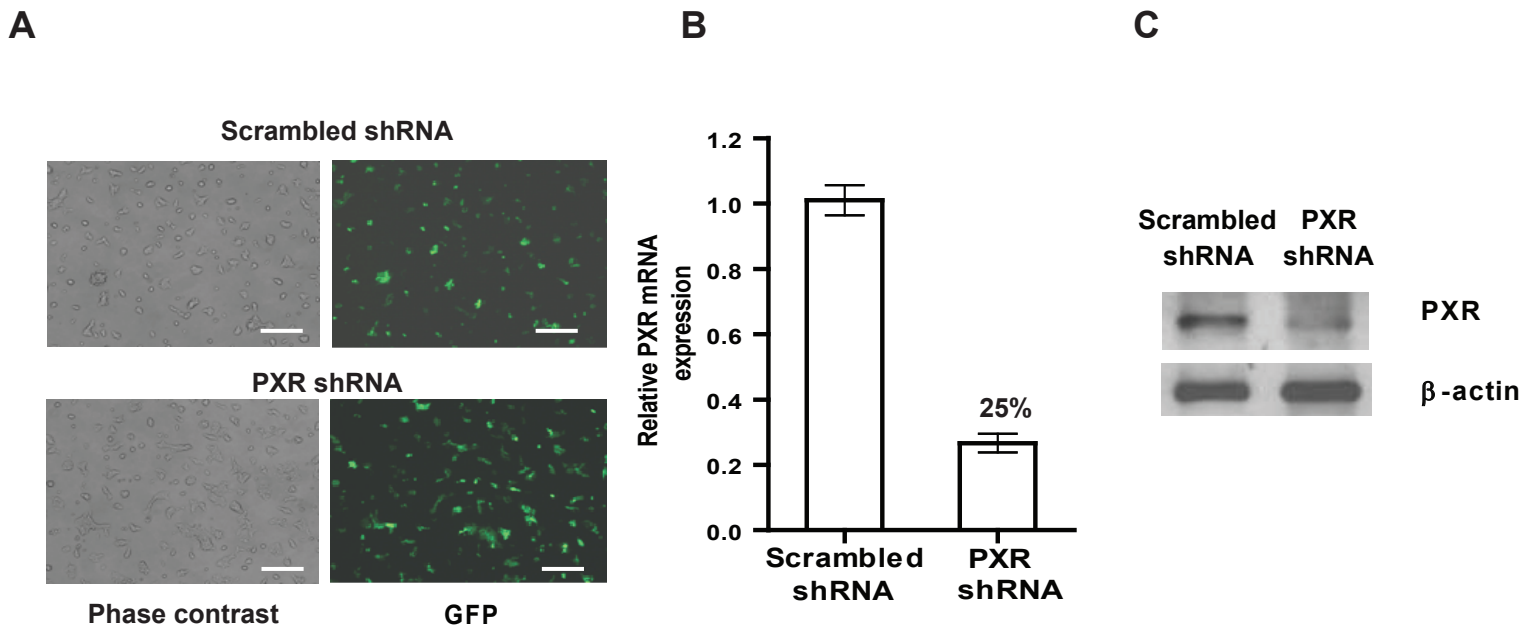

Supplemental Figure 1. PXR knockdown in LS174T cells. (**A**) LS174T cells transduced with scrambled and PXR shRNA with images captured under appropriate filters (Phase contrast and GFP). Scale bar, 100μm. (**B**) Real-time QPCR for PXR in cells expressing Scrambled shRNA or PXR shRNA. (**C**) Immunoblot of nuclear extract (100μg/lane) from cells transduced with scrambled shRNA and PXR shRNA. Data presented as mean ± SEM.

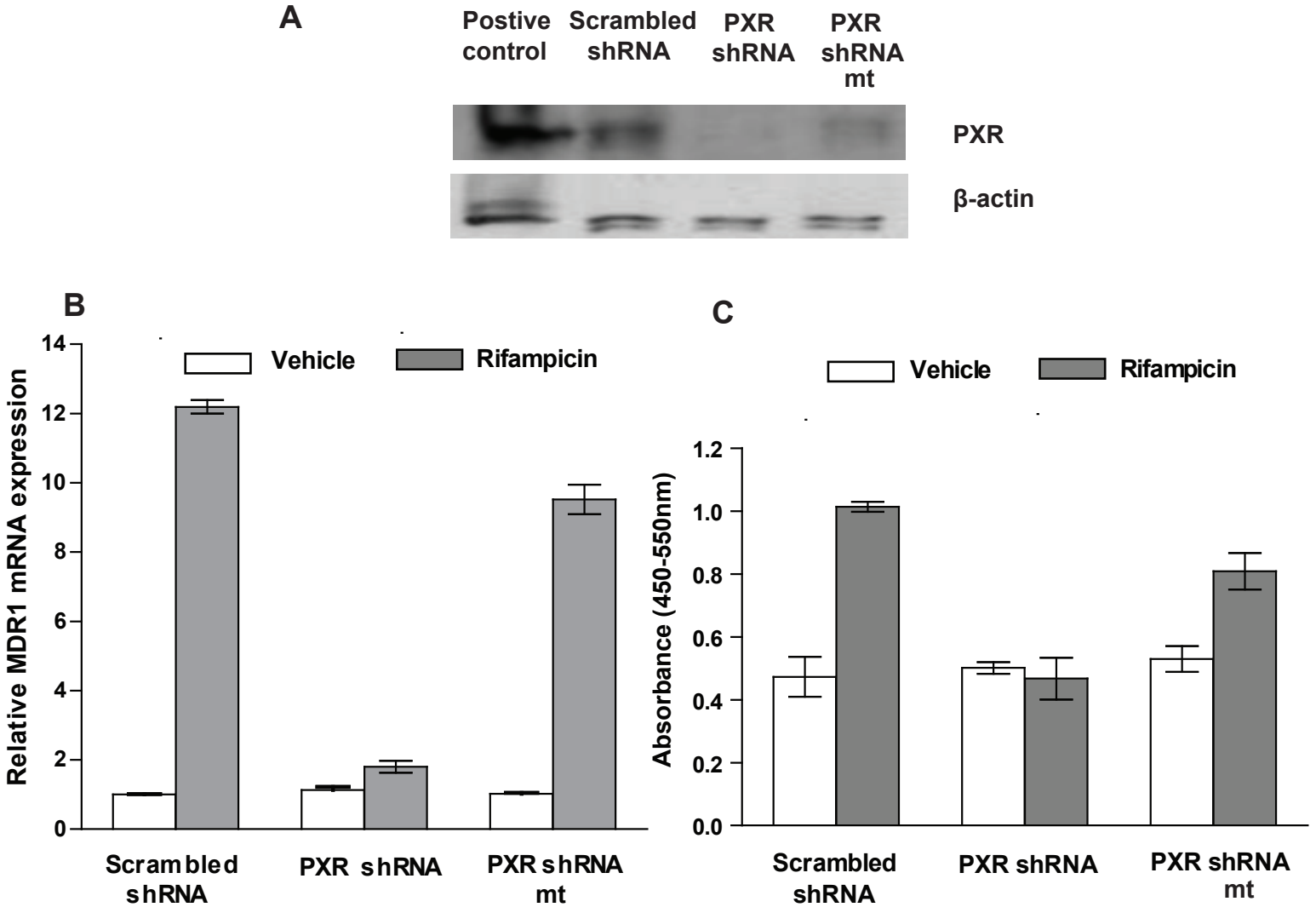

Supplemental Figure 2. Rescue of PXR phenotype in LS174T cells with PXR silent mutants. (**A**) Immunoblot of nuclear extract (100µg/lane) from cells transduced with Scrambled shRNA, PXR shRNA or PXR silent mutant (mt) expression plasmid. Positive control was nuclear extract (100µg/lane) from pSG5-PXR transfected 293T cells. β-actin served as loading control. (**B**) Real-time QPCR for MDR1 mRNA expression in cells expressing Scrambled shRNA, PXR shRNA, or PXR silent mutant (PXR shRNA mt). LS174T cells were exposed to vehicle control (0.2% DMSO) or rifampicin (10µM) for 48h and thereafter, total RNA was isolated. (**C**) BrdU labeling based proliferation assay of LS174T cells expressing Scrambled shRNA, PXR shRNA, or PXR shRNA silent mutant (PXR shRNA mt). LS174T cells were exposed to vehicle (0.2% DMSO) or rifampicin (10µM) for 48h. The data is shown as absolute absorbance values (dual spectra 450-550 nm). (**B**, **C**) n = 3 in triplicate. Data presented as mean ± SD.

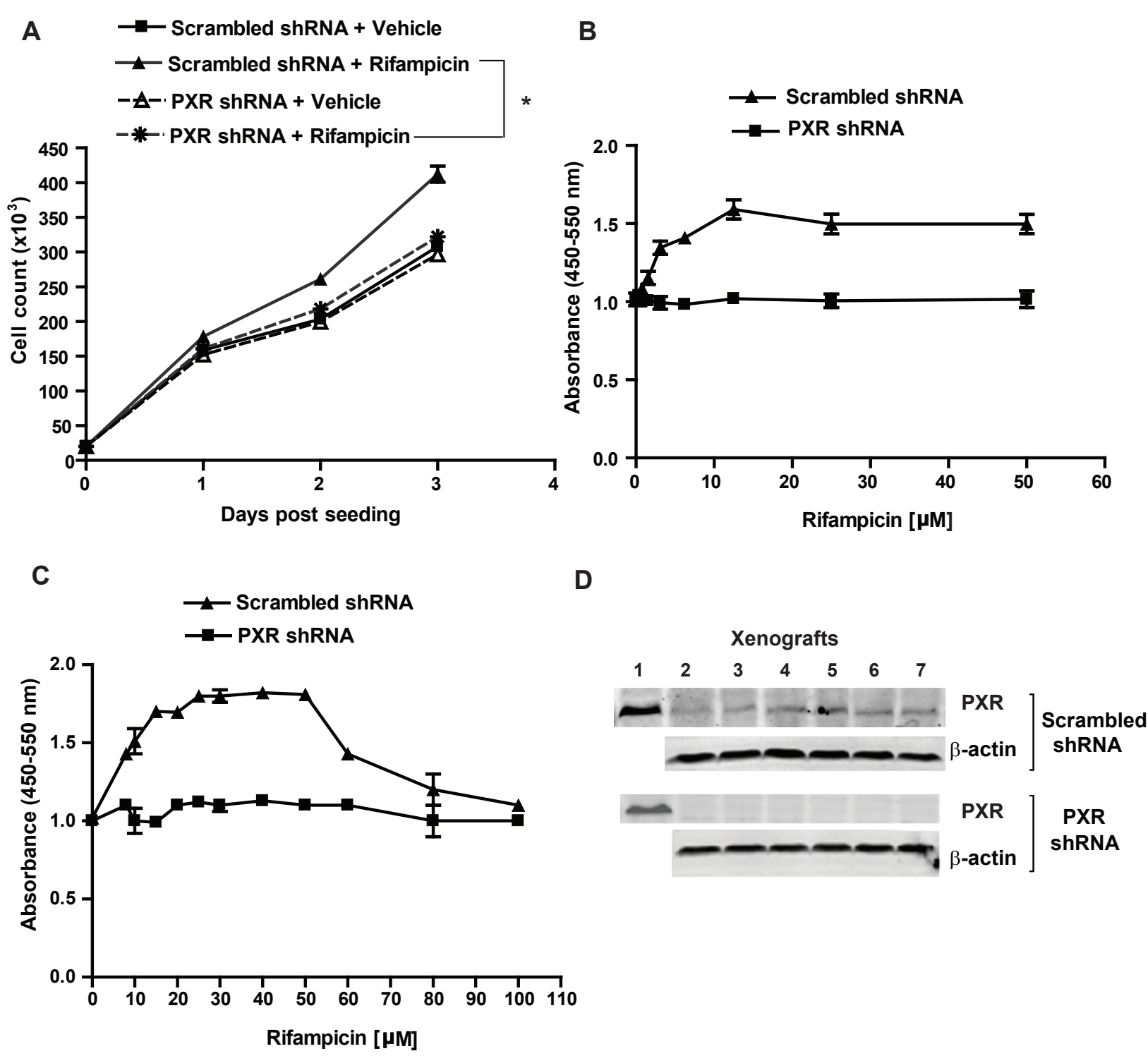

Supplemental Figure 3. PXR activation induces proliferation of colon cancer cells. (**A**) Doubling time of scrambled shRNA and PXR shRNA-transduced LS174T cells treated with either rifampicin or 0.2% DMSO (rifampicin vehicle); n = 8 with six replicates each. Proliferation (BrdU) assay of (**B**) LoVo and (**C**) HCT 116 cells expressing either scrambled shRNA or PXR shRNA. The cells had been treated with either rifampicin or 0.2% DMSO (vehicle). The data is shown as absolute absorbance values (dual spectra taken at 450nm and 550 nm). Data presented as mean ± SD. (**B, C**) n = 4 in triplicate. * $P < 10^{-5}$ (**D**) Immunoblot analysis of PXR expression in tumors harvested from mice inoculated with cells expressing scrambled and PXR shRNA as shown in the manuscript Figure 1. Lane 1 is positive control: nuclear extract (100μg/lane) from pSG5-PXR transfected 293T cells. Lanes 2-7 represent individual randomly selected tumors.

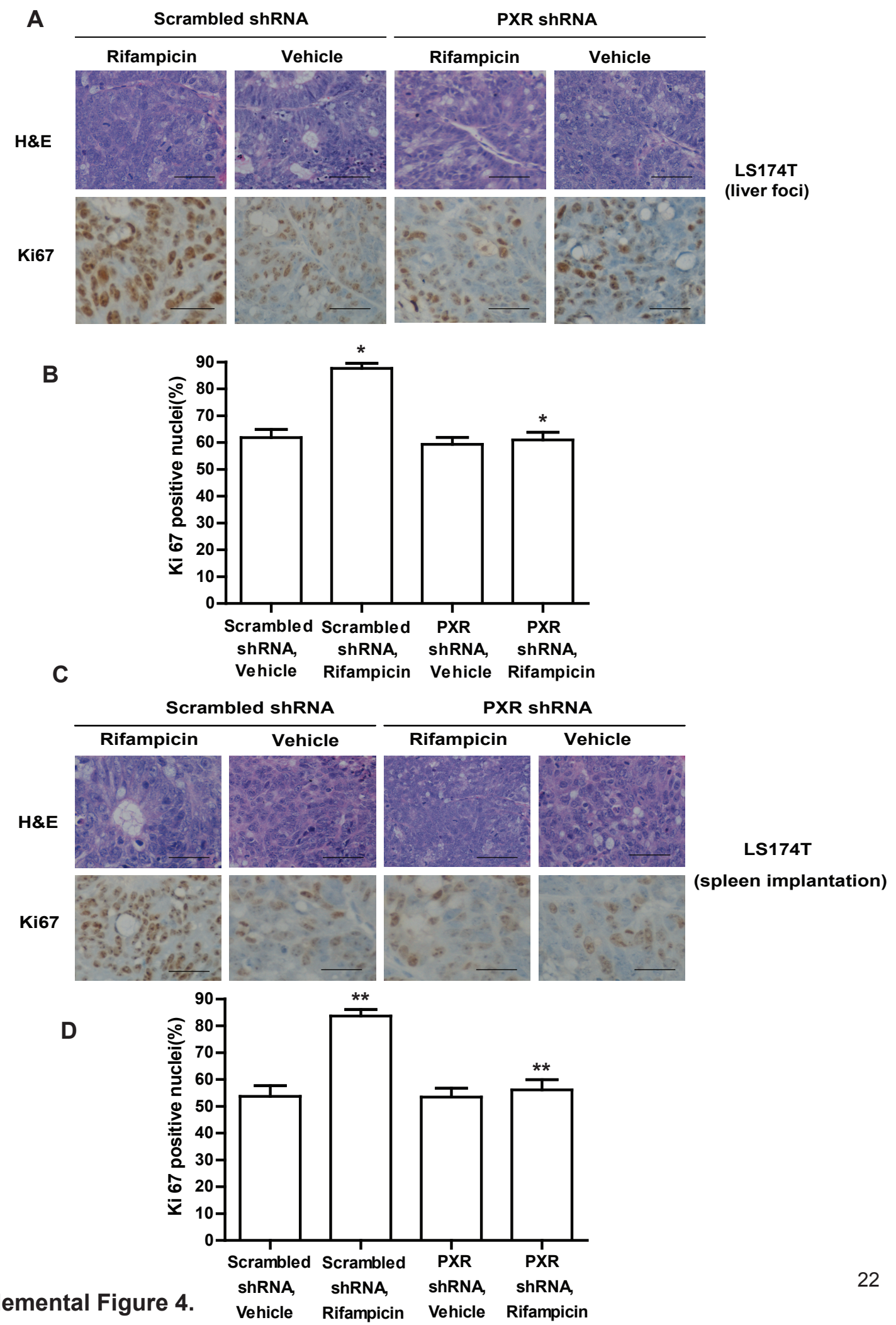

Supplemental Figure 4.

Supplemental Figure 4. PXR activation on LS174T cells promotes cell proliferation in primary and metastatic foci in vivo*.* Representative hematoxylin/eosin (H&E) stain and Ki67 immunostaining of tumor nodules from (**A**) liver and (**C**) spleen tissues from mice injected with LS174T cells transduced with Scrambled shRNA or PXR shRNA (n=24/group). (Original magnification: x20; Scale bar, 50 μm) Ki67 positive nuclei count in (**B**) liver tumor and (**D**) spleen nodules was scored in 10 high-power fields (HPF) by dividing the total number of positive-nuclei with the total number of nuclei counted and then expressed as a percentage (x 100). Data presented as mean ± SD, *, ** $P < 0.05$.

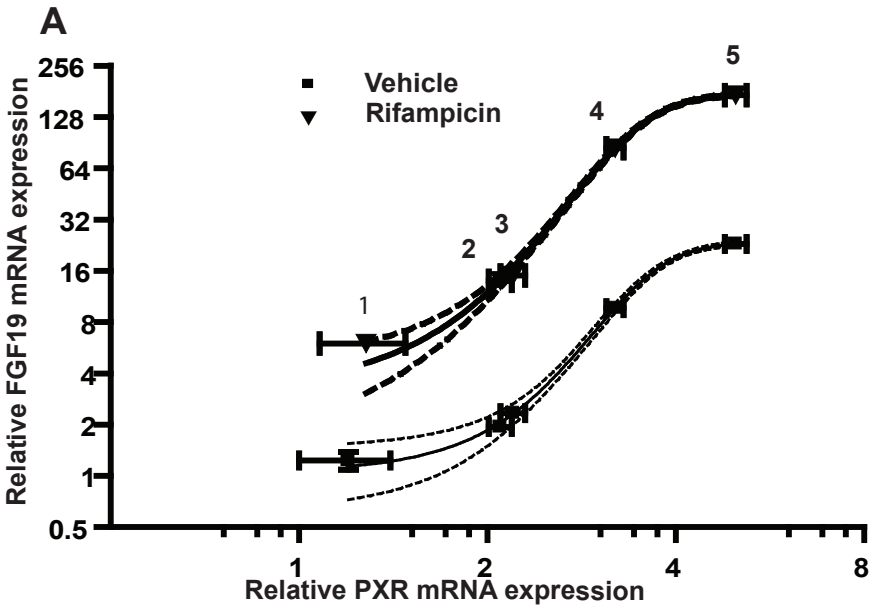

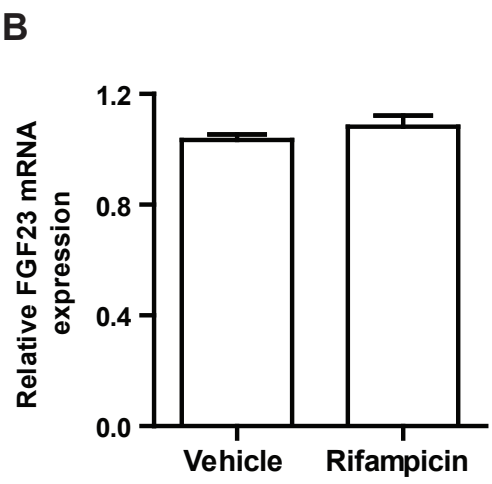

Cell lines	β actin		FGF 19	
	DMSO	Rifampicin	DMSO	Rifampicin
1- HCT116	22.231	22.518	36.221	34.221
2- SW948	22.253	22.447	35.252	32.784
3- SW403	22.115	22.460	34.694	32.508
4- LoVo	20.388	20.820	31.136	29.571
5- LS174T	20.641	20.474	30.204	27.101

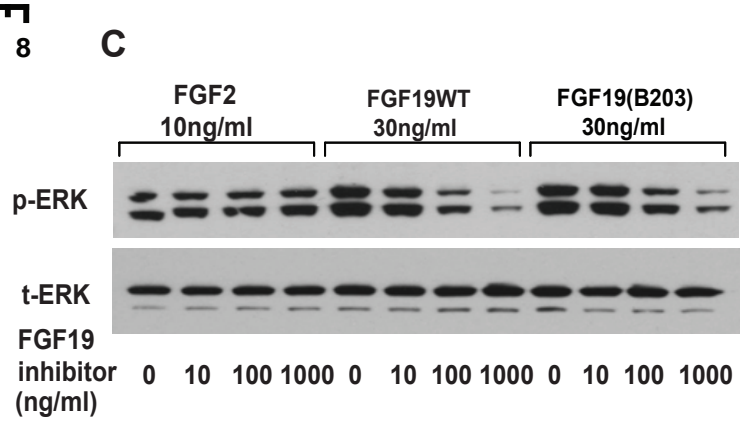

Supplemental Figure 5. Relationship between FGF19 and PXR mRNA expression in colon cancer cells. (**A**) Real-time QPCR of FGF19 mRNA in the colon cancer cell lines HCT116, SW948, SW403, LoVo, and LS174T after cell stimulation with either rifampicin (10μM) or 0.2% DMSO (rifampicin vehicle) for 48h. Table indicates average Ct values for β-actin and FGF19 in respective cell lines as treated. Data presented as mean (range). Solid line, fitted curve; dashed line 95% confidence limits (**B**) Real-time QPCR of FGF23 mRNA in parental LS174T cells treated with either rifampicin (10μM) or 0.2% DMSO (vehicle). Data presented as mean ± SEM. (**C**) FGF19 inhibitor blocks activation of intracellular FGF signaling by FGF19 protein but not FGF2. H4IIE cells were incubated with FGF19 or FGF2 protein and/or FGF19 inhibitor (C-terminal peptide of FGF19; aa# 171 - 216) at the indicated concentrations for 15 minutes. Cell lysates were subjected to immunoblot analysis using antibodies against ERK1/2 (t-ERK) or phosphorylated ERK1/2 (p-ERK) as previously described (17,18) [Data in panel (**C**) are for review purpose only and will be published in a separate study by Goetz et al.; FGF19WT and B203 represent two different preparations of FGF19 protein]. (**A**, **B**) n = 3 in triplicate.

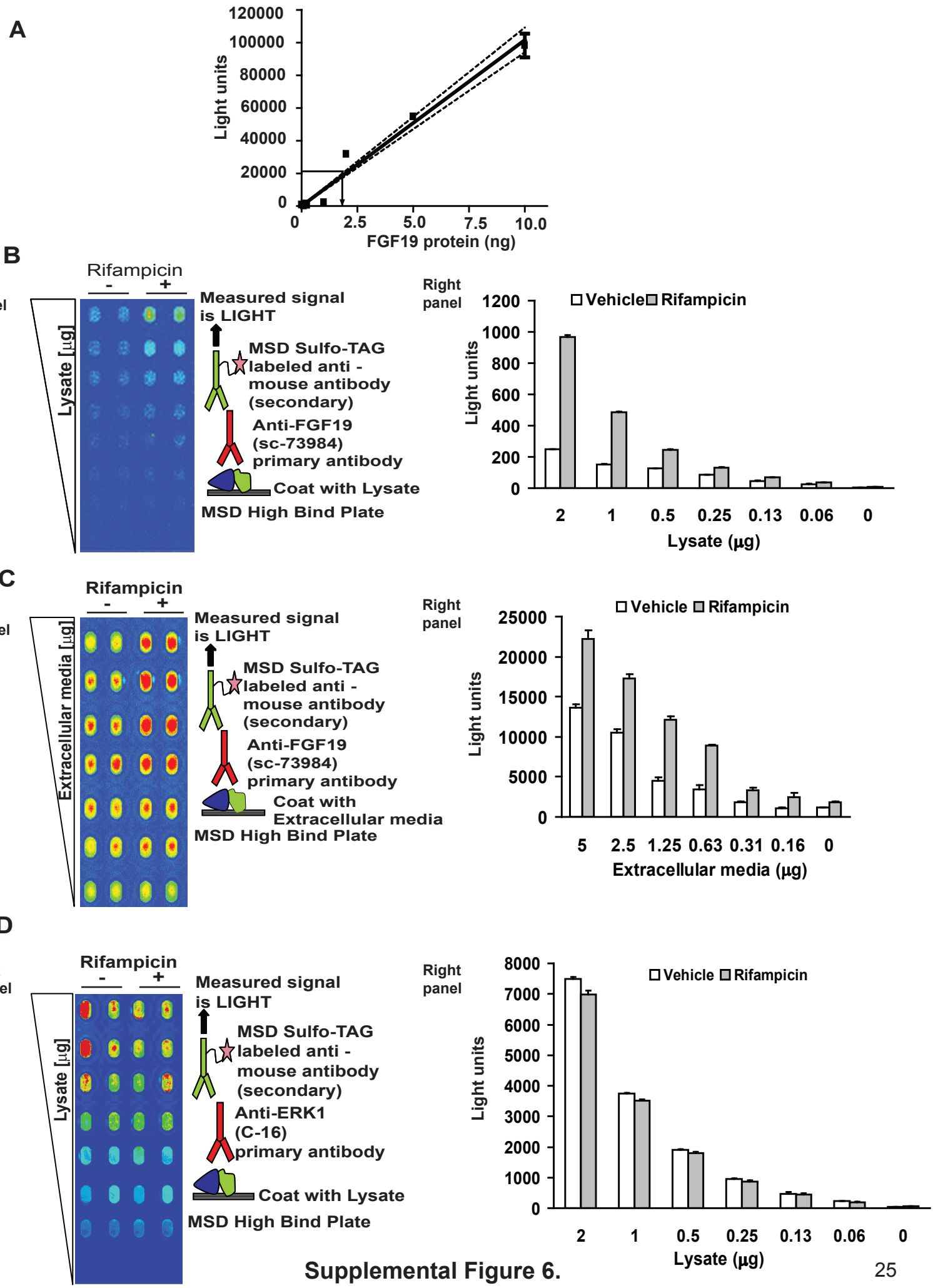

Supplemental Figure 6.

Supplemental Figure 6. Chemiluminescence method of detecting FGF19 and total ERK in lysate and extracellular media of the colon cancer cell line LS174T. Plates (96) wells were treated with a concentration gradient of LS174T cell lysate or extracellular media after the cells had been treated with either rifampicin or 0.2% DMSO (rifampicin vehicle) for 48 h. *Left panels*, show luminescence upon addition of secondary antibody (see cartoon of the assay). These assays were performed once in duplicate using FGF19 antibody and total ERK antibody. (**A**) Standard curve of FGF19 protein. Black arrow shows amount of FGF19 protein secreted into conditioned media (5μl) of LS174T cells upon stimulation with rifampicin. Light units plotted as a function of (**B** and **D**) LS174T cell lysate, (**C**) Extracellular serum-free media, (**D**) LS174T cell lysate using ERK antibody as loading controls. Data presented as mean + highest value obtained in the duplicate experiment.

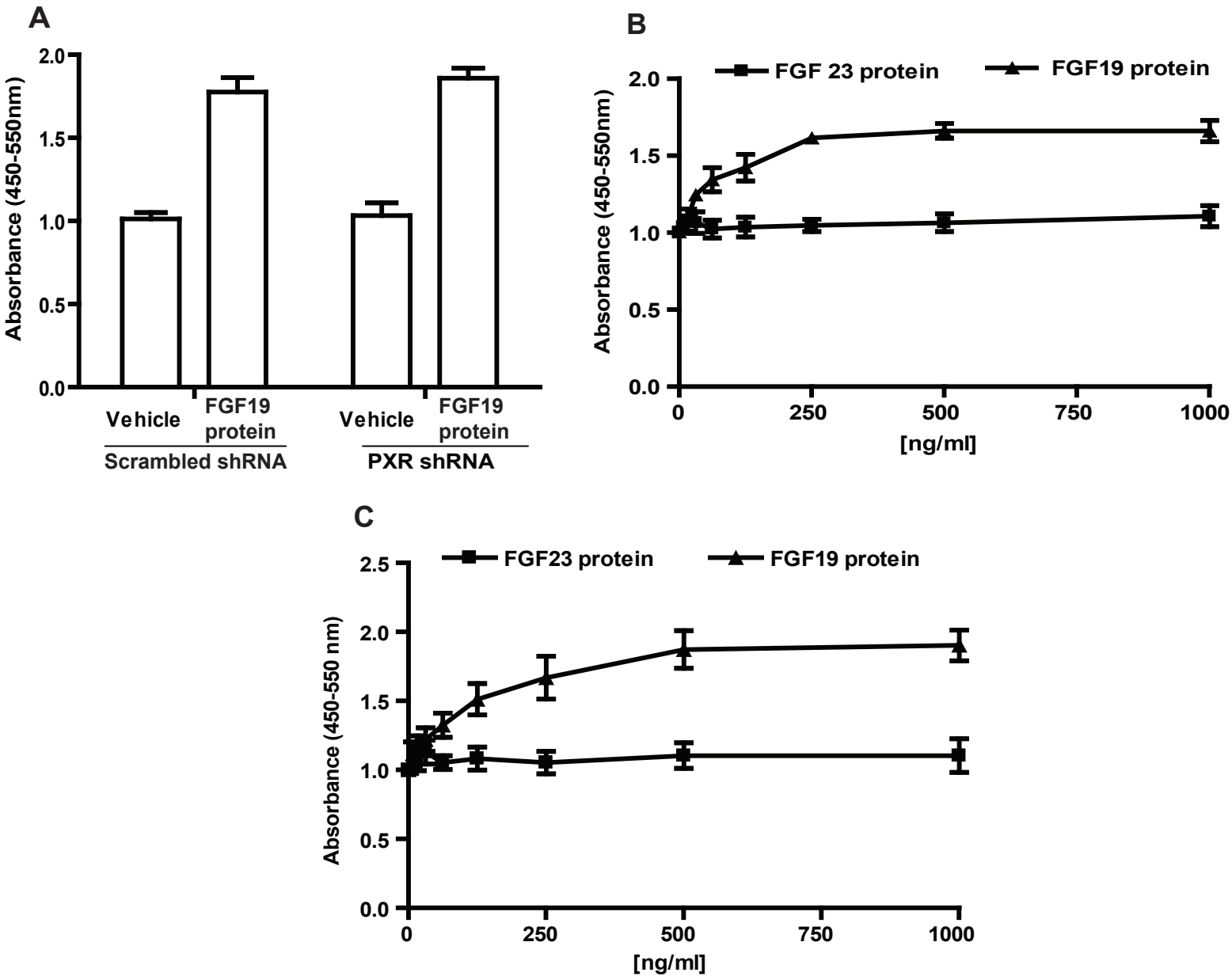

Supplemental Figure 7. Proliferation (BrdU) assay of (**A**) LS174T cells (scrambled and PXR shRNA) (**B**) HCT 116 and (**C**) LoVo cells treated with either FGF19 (0-1000ng/ml), FGF23 (0-1000 ng/ml) or HEPES buffer (2.5µl) (vehicle). The data is shown as absolute absorbance values (dual spectra taken at 450nm and 550 nm). Data presented as mean ± SEM. (**A**-**C**) n = 4 in triplicate.

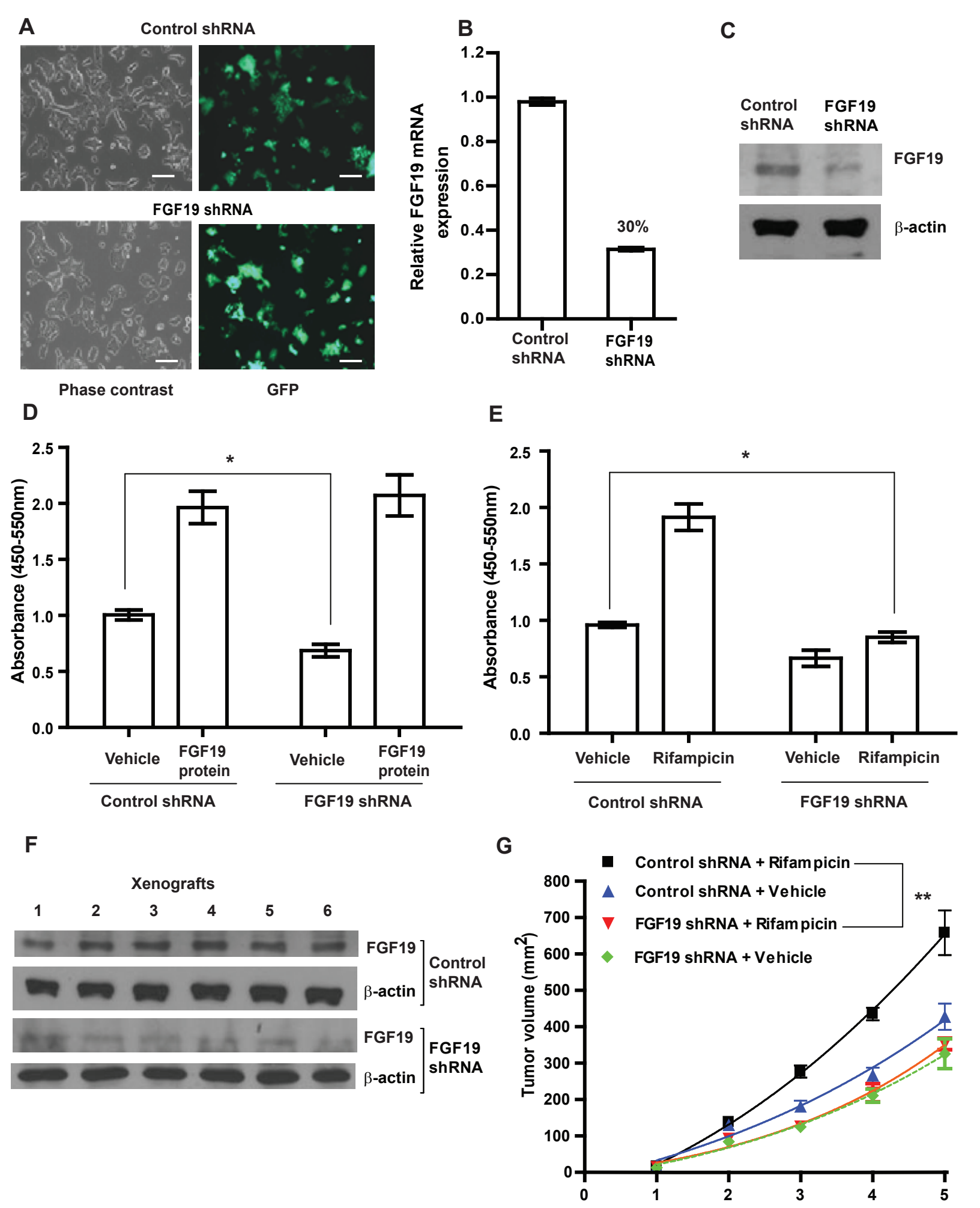

Supplemental Figure 8.

Supplemental Figure 8. FGF19 knockdown in LS174T cells. (**A**) LS174T cells transduced with control shRNA-Lenti-GFP and FGF19 shRNAmir's with images captured under appropriate filters (Phase contrast and GFP). Scale bar, 50 μm. (**B**) Real-time QPCR for FGF19 in cells expressing control shRNA or FGF19 shRNA; n = 3 in triplicate. (**C**) Immunoblot of FGF19 in nuclear extract (200μg/lane) from cells transduced with control shRNA and FGF19 shRNAmir's. Proliferation (BrdU) assay of LS174T cells expressing control shRNA and FGF19 shRNAmir's exposed to (**D**) vehicle (HEPES buffer) or FGF19 (1000ng/ml) or (**E**) vehicle (0.2% DMSO) or Rifampicin (10μM) for 48 h. The data is shown as absolute absorbance values (dual spectra 450-550 nm); n = 3 in triplicate. (**F**) Immunoblot of FGF19 from tumors harvested from cell lines implanted from (**A**) at week 5 (when all animals were euthanized). (**G**) LS174T cells as in (**A**) were grown as xenografts (n= 12 per group) in 6-8 week old nude mice, tumors were treated with rifampicin or vehicle (IP, 3 days/week). All data presented as mean ± SEM. * , ** $P < 0.05$.

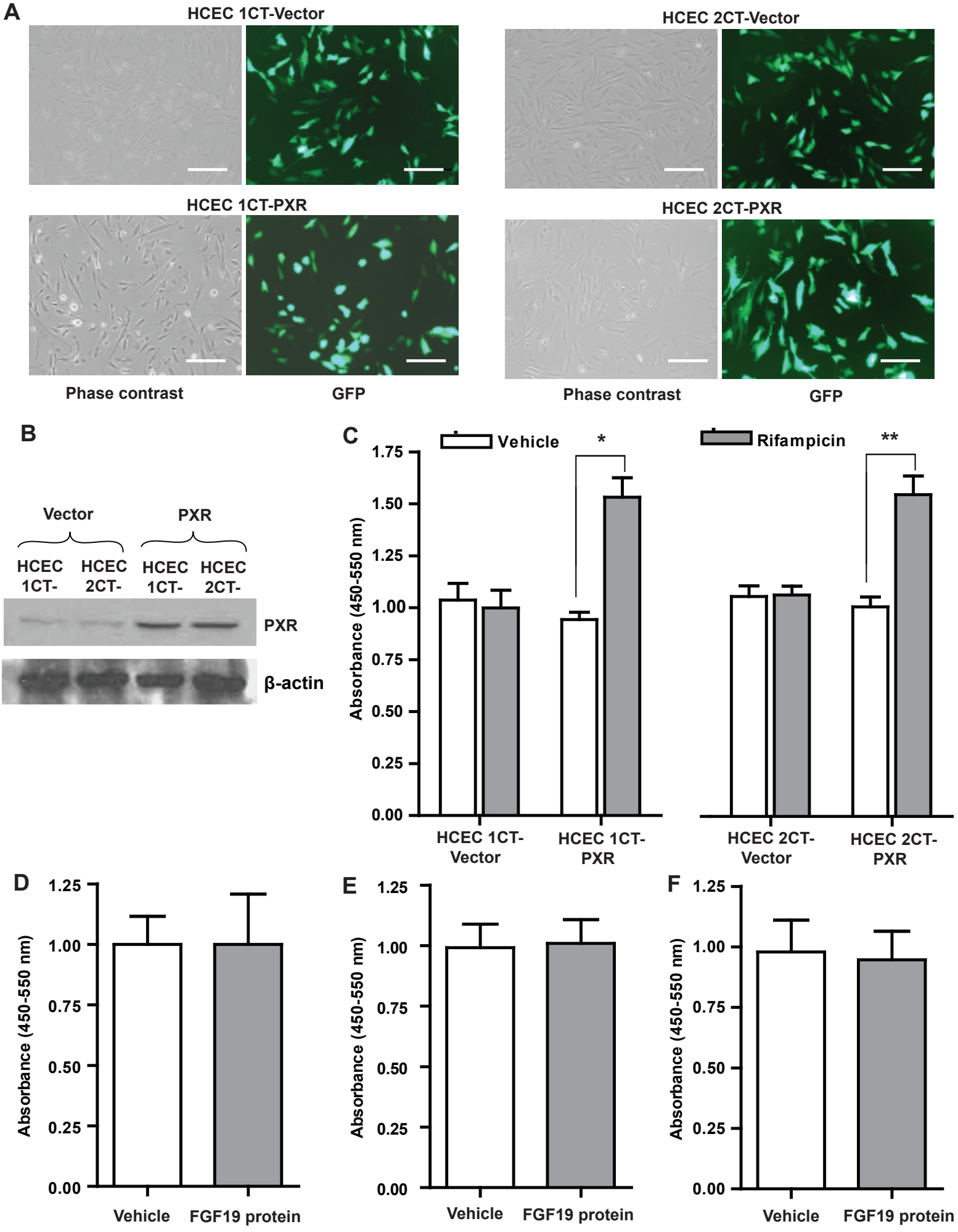

Supplemental Figure 9.

Supplemental Figure 9. Effect of FGF19 on HIEC and HCECs (immortalized human colon cells) in vitro. (A) HCEC 1CT and HCEC 2CT cells transfected with pEGFPC1 vector (HCEC 1CT/2CT-vector) or pEGFPC1-hPXR (HCEC 1CT/2CT -PXR), images captured under appropriate filters (Phase contrast and GFP). Scale bar, 100 μm. (**B**) Representative PXR immunoblot of pooled HCEC 1CT/2CT-vector and HCEC 1CT/2CT -PXR cells nuclear extract (200 μg/lane). (**C**) Proliferation (BrdU) assay of HCEC 1CT and 2CT cells (vector and PXR transfected) that had been treated for 48 h with either rifampicin (10μM) or vehicle (0.2% DMSO). Proliferation (BrdU) assay of (**D**) HIE cells (**E**) HCE 1CT and (**F**) HCE 2 CT cells treated with either FGF19 (1000ng/ml) or HEPES buffer (2.5μl) (vehicle) for 48 h. Proliferation data is shown as absolute absorbance values (dual spectra taken at 450nm and 550 nm); n = 3 in quadruplicates. Data presented as mean ± SEM. **P* < 0.051, ***P* < 0.05.

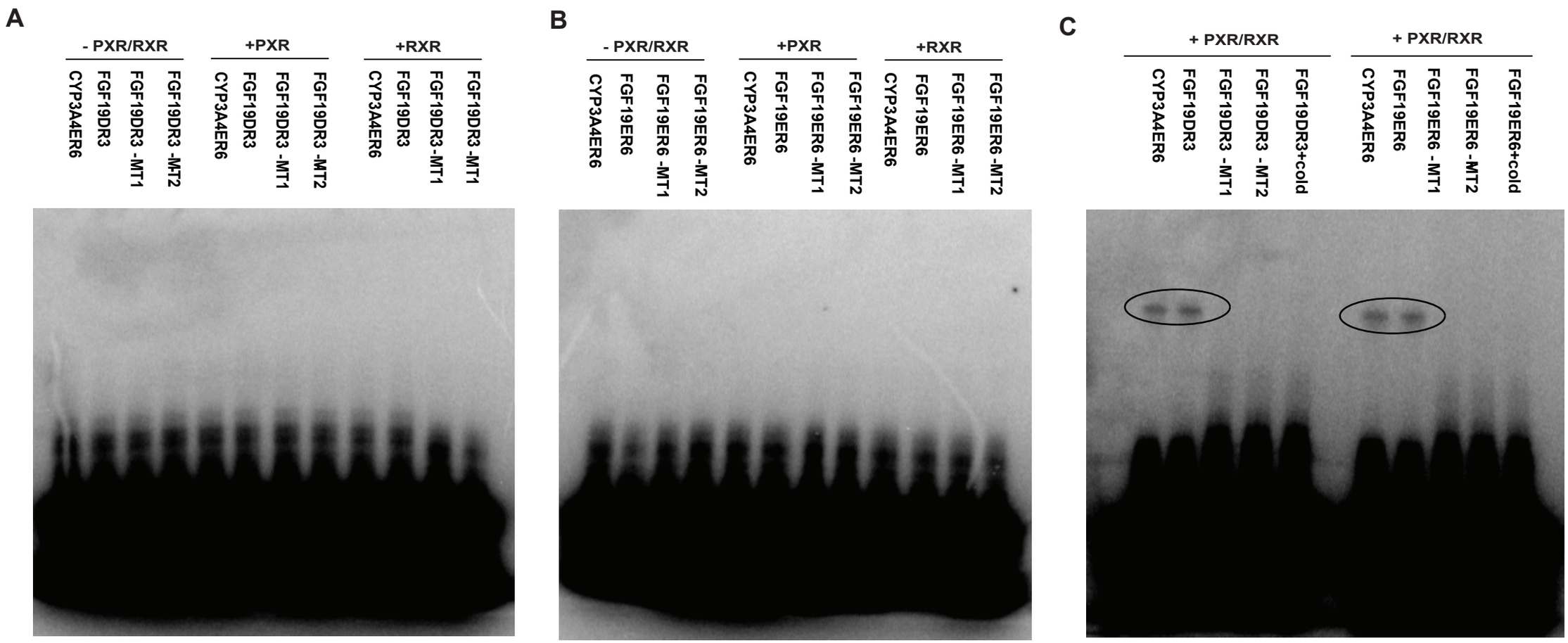

Supplemental Figure 10. Electromobility shift assay (EMSA) of PXR (see Supplemental Methods). Lack of binding of FGF19 probe sequences incorporating proximal (A) DR3 or (B) ER6 elements when incubated with PXR or RXR alone. RXR heterodimer complexes (with PXR) bind to (C) DR3 and ER6. The black circles indicates PXR: RXR bound to *CYP3A4 (ER6) [3A4/ER6] and FGF19 (DR3) oligo. and FGF19 (ER6) oligo. MT1 and MT2 represent oligos with mutant DR3 or ER6 elements. Cold oligo (50x), 50-fold excess of unlabeled FGF19 (DR3) or FGF19 (ER6) oligos, respectively.

A

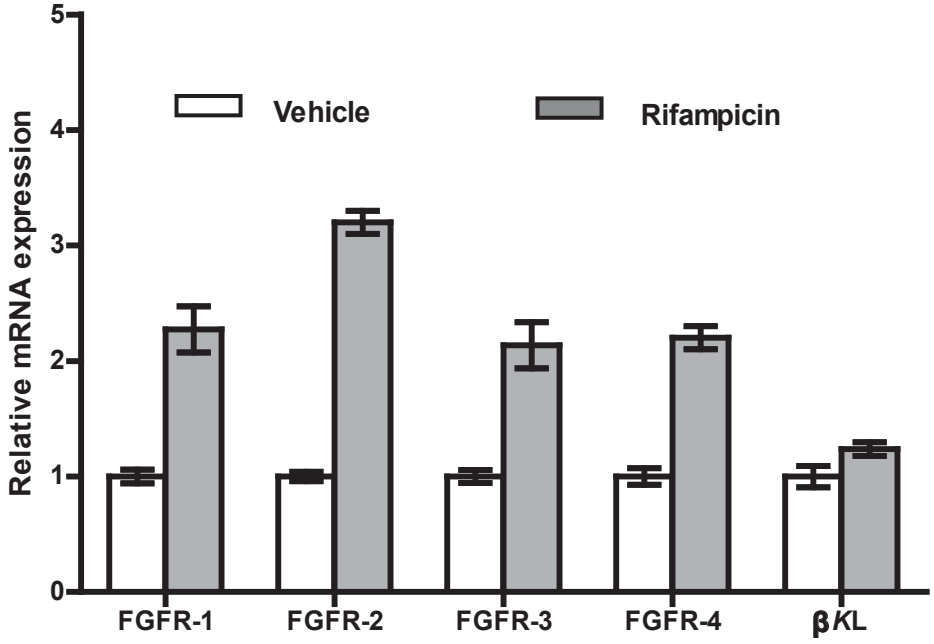

	FGFR-1		FGFR-2		FGFR-3		FGFR-4		βKL	
	β-actin	FGFR1	β-actin	FGFR2	β-actin	FGFR3	β-actin	FGFR4	β-actin	βKL
Vehicle	21.80	29.09	21.85	29.75	22.18	31.34	22.024	27.253	22.481	31.32
Rifampicin	22.6	28.72	22.3	28.46	22.3	30.5	22.497	26.451	22.448	31.08

B

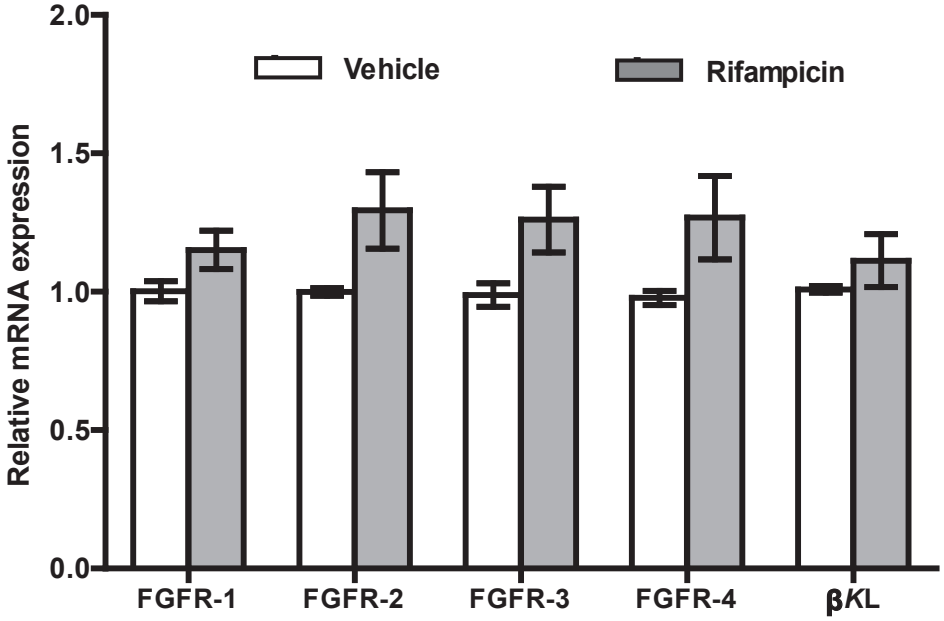

	FGFR-1		FGFR-2		FGFR-3		FGFR-4		βKL	
	β-actin	FGFR1	β-actin	FGFR2	β-actin	FGFR3	β-actin	FGFR4	β-actin	βKL
Vehicle	20.66	29.95	20.29	31.57	20.64	31.19	20.26	26.40	20.41	31.07
Rifampicin	20.91	29.82	20.30	31.09	20.71	30.70	20.30	26.10	20.55	30.76

Supplemental Figure 11. Expression of FGFR1-4 and β*K*lotho in LS174T cells and human colon cancer xenotransplants. (**A**) Real Time-QPCR for FGFR 1-4 and β*K*lotho mRNA in LS174T cells treated with 0.2% DMSO or rifampicin (10μM); n = 4 in triplicate. (**B**) Primary human tumors (n=4 samples) were passaged once in mice as heterotransplants (treated with 30% polyethylene glycol x 3 injections; n=4) and subsequently re-passaged twice more (treated with rifampicin 40 mg/kg/day IV for 3 consecutive days; n=4 samples). The mice were sacrificed on day 4, tumors extracted and immediately processed for isolation of total RNA. The samples were then simultaneously processed for real-time QPCR. Gene expression changes were calculated using comparative Ct method with β-actin as the reference gene and vehicle as the calibrator. n = 4 in triplicate. Data presented as mean ± SEM.

References

1. Levy E, et al. Human crypt intestinal epithelial cells are capable of lipid production, apolipoprotein synthesis, and lipoprotein assembly. *J Lipid Res.* 2000; 41(1):12-22.
2. Goetz R, et al. Isolated C-terminal tail of FGF23 alleviates hypophosphatemia by inhibiting FGF23-FGFR-Klotho complex formation. *Proc Natl Acad Sci U S A.* 2010;107(1):407-412.
3. Goetz R, et al. Molecular insights into the klotho-dependent, endocrine mode of action of fibroblast growth factor 19 subfamily members. *Mol Cell Biol.* 2007; 27 (9):3417-3428.
4. Desnoyers LR, et al. Targeting FGF19 inhibits tumor growth in colon cancer xenograft and FGF19 transgenic hepatocellular carcinoma models. *Oncogene.* 2008; 27 (1):85-97.
5. Gupta D, et al. Expanding the roles for pregnane X receptor in cancer: proliferation and drug resistance in ovarian cancer. *Clin Cancer Res.* 2008; 14 (17):5332-5340.
6. Bhalla S, Ozalp C, Fang S, Xiang L, and Kemper JK. Ligand-activated pregnane X receptor interferes with HNF-4 signaling by targeting a common coactivator PGC-1alpha. Functional implications in hepatic cholesterol and glucose metabolism. *J Biol Chem.* 2004; 279 (43):45139-45147.
7. Rao S, Procko E, Shannon MF. Chromatin remodeling, measured by a novel real-time polymerase chain reaction assay, across the proximal promoter region of the IL-2 gene. *J Immunol.* 2001; 167(8):4494-4503.
8. Bookout AL, Mangelsdorf DJ. Quantitative real-time PCR protocol for analysis of nuclear receptor signaling pathways. *Nucl Recept Signal.* 2003; 1e012.
9. Li LC, Dahiya R. MethPrimer: designing primers for methylation PCRs. *Bioinformatics.* 2002; 18(11):1427-1431.
10. Roig AI, et al. Immortalized epithelial cells derived from human colon biopsies express stem cell markers and differentiate in vitro. *Gastroenterology.* 2010; 138 (3):1012-1021 e1011-1015.
11. Huang H, et al. Inhibition of drug metabolism by blocking the activation of nuclear receptors by ketoconazole. *Oncogene.* 2007; 26 (2):258-268.
12. Sun D, Melegari M, Sridhar S, Rogler CE, and Zhu L. Multi-miRNA hairpin method that improves gene knockdown efficiency and provides linked multi-gene knockdown. *Biotechniques.* 2006; 41 (1):59-63.
13. Nelson JD, Denisenko O, and Bomsztyk K. Protocol for the fast chromatin immunoprecipitation (ChIP) method. *Nat Protoc.* 2006; 1 (1):179-185.
14. Foster SL, Hargreaves DC, and Medzhitov R. Gene-specific control of inflammation by TLR-induced chromatin modifications. *Nature.* 2007; 447 (7147):972-978.
15. Thalheimer A, et al. The intraportal injection model: a practical animal model for hepatic metastases and tumor cell dissemination in human colon cancer. *BMC Cancer.* 2009; 9:29.
16. Williams G, et al. Mutagenesis studies of interleukin-8. Identification of a second epitope involved in receptor binding. *J Biol Chem.* 1996; 271 (16):9579-9586.
17. Kurosu H, et al. Regulation of fibroblast growth factor-23 signaling by klotho. *J Biol Chem.* 2006; 281 (10):6120-6123.
18. Kurosu H, et al. Tissue-specific expression of betaKlotho and fibroblast growth factor (FGF) receptor isoforms determines metabolic activity of FGF19 and FGF21. *J Biol Chem.* 2007; 282 (37):26687-26695.